Research Article Vol. 28, No. 9 / 27 April 2020 / Optics Express 12518
Optics EXPRESS

Research on the new detection method of suppressing the skylight background based on the shearing interference and the phase modulation

LEI DONG AND BIN WANG*

Changchun Institute of Optics, Fine Mechanics and Physics, Chinese Academy of Sciences, Changchun 130033, China
*175969722@qq.com

Abstract: In order to effectively suppress the effect of the skylight background on the detection performance of the optical telescope and make it have the advantages of the all-time operation and the high star-magnitude detection, a new detection method based on the shearing interference and the phase modulation is proposed in this paper. This method utilizes the discrepancy of the spatial coherence between the target (smaller size) and the skylight background (larger size). By adjusting the shearing amount reasonably, the target light can form the interference fringes, while the skylight background cannot. Then, the phase modulation technique is used to form the moving interference fringes over the detector. Afterward, the periodical electrical signal is formed by the photoelectrical conversion of the detector. Finally, the weak signal detection equipment can be used to extract the target signal from the skylight background noise. This paper introduces the scheme design and the theoretical analysis of the new detection method and also presents the detection performance simulation of this new method.

1. Introduction

The optical searching and tracking telescope is a general-purpose equipment which is widely used for the precise pointing of laser beams, the positioning and attitude keeping of flight platforms and the high precise tracking and aiming of large aperture telescopes. The existing optical searching and tracking systems are more or less affected by the sun and the skylight background, so their detection time, detection performance and measurement accuracy are seriously restricted. There are several methods to suppress the skylight background noise, while the existing methods (mainly including: the field of view (FOV) control method [1], the spectral filtering method [2-4] and the polarization filtering method [5,6]) have their own limitations. For the FOV control method, the drawbacks are that the FOV is too little and that the suppression of the strong skylight background is poor. For the spectral filtering method, the drawback is that when the spectral distribution of the target is similar to that of the skylight background, it is difficult to distinguish the peaks of the spectral energy between the target and the skylight background. For the polarization filtering method, it is generally necessary to estimate in advance the discrepancy of the polarization states between the target and the skylight background, while the specific implementation is more complex because of the changes of the polarization states according to the orbital motion and the attitude change of the target as well as the change of the sun altitude angle, etc..

In order to circumvent the above problems, Daniel N. Held proposed a star tracker based on the optical interference and the phase modulation [7], which is used to suppress the influence of strong skylight background in the daytime to improve the detection performance for finding the dark stars. This new device ingeniously utilizes the discrepancy of the spatial coherence of distant light fields between the target and the skylight background [8], introduces the periodical change

#386752 https://doi.org/10.1364/OE.386752
Journal © 2020 Received 26 Dec 2019; revised 7 Mar 2020; accepted 22 Mar 2020; published 13 Apr 2020

Optics EXPRESS

of the target light by the phase modulation and then uses the weak signal detection technique [9,10] to evidently improve the signal-to-noise ratio (SNR) of the target light, so as to realize the detection of the dark target in the strong skylight background.

However, Daniel N. Held's device has some deficiencies in the real applications. The main problems are that it is difficult to achieve the high contrast optical interference and that it only has low aperture utilization. The aperture of the electro-optical modulator is limited (generally less than 1 cm) and the outline dimension of the electro-optical modulator (about 1 ~ 3 cm) is generally larger than its aperture. The above limits result in a larger center distance (possibly greater than 3 cm) between the two light paths. In general, the far-field coherent region of a short-range (about 100 km) target (the size about 1 m) is about 5 cm (the central wavelength is 532 nm). If the center distance between the two light paths is more than 3 cm, the contrast of the interference fringes is very low and it is easy to be submerged by the background noise. In addition, the above device belongs to the wavefront-splitting interference. The drawback of this interference is that the center distance between the two light paths cannot be less than the diameter of each light path. As the diameter of each light path is at most equal to half of the size of the coherent region, this device only has low aperture utilization (less than 50%).

In this paper, a new detection method based on the shearing interference and the phase modulation is proposed. The working principle of the new method is basically the same as that of the device proposed by Daniel N. Held. The difference is that the new method replaces the wavefront-splitting interference with the amplitude-splitting interference (the shearing interference), which overcomes the above deficiencies of the device proposed by Daniel N. Held. In our new method, the original two electro-optical modulators are replaced by the shearing interferometer (composed of two Ronchi phase gratings) and the center distance (the shearing amount) between the two shearing beams can be properly adjusted (generally from zero to several centimeters), which can realize the interference of the lights from targets with different altitudes and sizes. In addition, because the center distance between the two beams is very close to zero, the aera in the far-field coherent region of the target can be fully utilized and the aperture utilization may be close to 100%.

The device based on the new shearing interference detection method can be placed on the ground-based, sea-based, or space-based platforms. It can realize the all-time detection and tracking of large telescopes, the all-time accurate pointing of laser beams, the all-time attitude control of aircrafts, etc.

2. Scheme design and working principle

The structural diagram of the new shearing interference detection system is shown in Fig. 1, including the shearing interferometer composed of two Ronchi phase gratings, the piezoelectric ceramics actuator (PZT), the beam shrinking system (also know as telescope), the detector and the weak signal detection equipment.

The working principle of the detection system is described as follows. The lights from the target and the skylight background (the mixed light) are incident on a shearing interferometer [11-14] composed of two same Ronchi phase gratings [15]. Grating 1 is parallel to grating 2 and there is a small angle of the grating lines between gratings 1 and 2. When the mixed light is normally incident on grating 1, the directions of the±1 order diffraction from grating 1 are symmetrically distributed on both sides of the optical axis. After the ± 1 order diffraction lights pass through grating 2, they become two parallel beams, forming two lateral-shearing beams. The center distance between the two parallel beams is equal to the shearing amount. These two beams are the copies of the mixed light, that is, the wavefront distributions of the two beams are exactly the same as that of the mixed light. Based on the Van Cittert - Zernike theorem [8], the target light can form interference fringes by reasonably selecting the shearing amount (which can be achieved by changing the distance between two gratings), while the skylight background

Optics EXPRESS

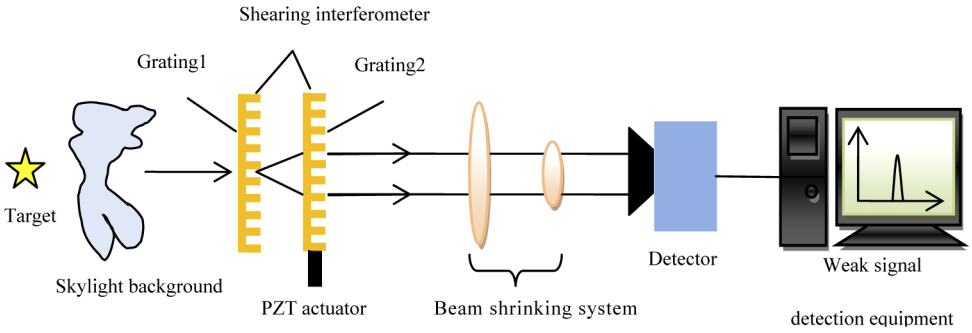

Fig. 1. Structural diagram of a new shearing interference detection system.

can't. The PZT actuator under grating 2 can achieve the periodical stretching movement, so that grating 2 moves back and forth along the beam shearing direction. This back-and-forth motion of grating 2 can cause the lateral (perpendicular to the optical axis) back-and-forth motion of the interference fringes. The function of the beam shrinking system is to compress the coverage area of the interference fringes, so that the energy of the interference fringes is more concentrated to improve the contrast of the fringes. In addition, it can also match the width of the fringe with the size of the pixel of the detector. When the width of the fringe is comparable to the size of the pixel, the periodical electrical signal will be generated after the fringes scanning across the pixel. When the SNR is low, the above electrical signal is submerged in the random electrical signals generated by the skylight background and other noises. Fortunately, the above periodical signal can be detected by the weak signal detection method.

3. Mathematical modeling

By the introduction of section 2, we know that the core of the new shearing interference detection method is to convert the target light into the periodical signal, so that it can be extracted from the random noises by the mature weak signal detection technique. For the convenience of the analysis and the simulation, we make the following assumptions.

(I) It is assumed that the target light is a monochromatic plane wave and that its propagation in the free space and the optical elements can be described by the scalar wave optics.

(II) It is assumed that the size of grating 2 is large enough, so the back-and-forth motion of grating 2 can be replaced by one-way motion. It can cause the continuous movement of interference fringes in one direction. The one-way scanning of interference fringes across the detector can produce a periodical signal, which is generally similar to the sinusoidal structure.

(III) It is assumed that the optimized shearing amount is used in the simulation, that is, the skylight background can't form the interference fringes, while the target can form the high contrast fringes. As the grating shearing interferometer can realize the continuous change of the shearing amount from zero to several centimeters, the optimized shearing amount can always be found by experiments.

(IV) It is assumed that the interference fringe formed by the shearing interferometer can match perfectly with the pixel of the detector, so there is no need to add the beam shrinking system.

(V) It is assumed that the detector signal generated by the illumination of skylight background is the Gaussian white noise and that this noise is far greater than other noises such as the

Optics EXPRESS

thermal noise, the low-frequency noise, etc. So there are only this noise and the photon fluctuation noise in the detection system. When the skylight background noise is larger than the amplitude of the target signal, the target signal will be submerged by the skylight background noise.

(VI) It is assumed that the weak signal detection method used in our simulation consists of the Fourier transform in the time domain and the narrow-band filtering in the frequency domain.

3.1. Generation model of the interference fringes of the target light

The physical process of the target light forming the moving interference fringes on the detector is as follows. The target light first passes through grating 1 and then diffracts between gratings 1 and 2. After that, this light passes through grating 2 and then diffracts between grating 2 and the detector. Finally, this light forms interference fringes on the detector. Grating 2 is controlled to move along the direction in the grating plane vertical to the grating lines, which causes the interference fringe pattern to scan across the pixels of the detector in one direction.

According to the wave optics theory, the expression of the light field on the detector can be obtained:

$$E_{fri} = F_{trans}^{-1}(F_{trans}(F_{trans}^{-1}(F_{trans}(E_{in} \cdot T_1) \cdot H_1) \cdot T_2) \cdot H_2), \tag{1}$$

In Eq. (1): E_{fri} is the light field on detector; $E_{in}$is the incident light field on the front surface of grating 1, which can be expressed as:

$$E_{in} = A_1 e^{i(\vec{k} \cdot \vec{r} + \phi_0)} = A_1 e^{i(ky \sin\theta + kz\cos\theta + \phi_0)}, \tag{2}$$

In Eq. (2): A_1 is the amplitude of the incident light; $\vec{k}$ is the wave vector; $\vec{r}$ is the position vector; $k = 2\pi/\lambda$ is the size of the wave vector; λ is the wavelength; y and z are the coordinate values, respectively; θ is the angle between the wave vector and the $z$axis and is the initial phase.

T_1 is the amplitude transmittance of grating 1, which can be expressed as:

$$T_1 = \begin{cases} 1 & y \in [nd, nd + \frac{d}{2}] \\ e^{i\pi} & y \in [nd + \frac{d}{2}, nd + d] \end{cases}, \tag{3}$$

In Eq. (3): the external dimensions of grating 1 are ignored and the phase difference between the convex and concave structures of grating 1 is assumed to be π; d is the grating period (or the grating constant) and $n \in (-\infty, +\infty)$ is an integer.

T_2 is the amplitude transmittance of grating 2, which can be expressed as:

$$T_2 = T_1 * \delta(y - vt), \tag{4}$$

In Eq. (4): $*$ represents the convolution operator; $\delta(y)$ is the unit impulse function (when$y = 0$,$\delta(y) = 1$ and others $\delta(y) = 0$); v is the one-way moving speed of grating 2 and t represents the time.

H_1 is the amplitude transfer function between gratings 1 and 2, which can be expressed as:

$$H_1 = e^{ikz_1} e^{-i\pi\lambda z_1 (f_x^2 + f_y^2)}, \tag{5}$$

In Eq. (5): z_1 is the distance between gratings 1 and 2; $f_x = x/\lambda z_1$ and $f_y = y/\lambda z_1$ are the spatial frequencies, respectively.

Optics EXPRESS

H_2 is the amplitude transfer function between grating 2 and the detector, which can be expressed as:

$$H_2 = e^{ikz_2} e^{-i\pi\lambda z_2(f_x'^2+f_y'^2)}, \tag{6}$$

In Eq. (6): z_2 is the distance between grating 2 and the detector; $f_x' = x/\lambda z_2$ and $f_y' = y/\lambda z_2$ are the spatial frequencies, respectively.

F_{trans} is the Fourier transform operator in space domain and F_{trans}^{-1} is the inverse Fourier transform operator in space domain.

The light intensity of interference fringes can be expressed as follows:

$$I_{fri} = E_{fri} \cdot E_{fri}^*, \tag{7}$$

In Eq. (7): I_{fri} is the light intensity on the detector and E_{fri}^* is the complex conjugation of the light field on the detector.

So far, we have obtained the mathematical model of the formation process of the interference fringes on the detector. The one-way motion of grating 2 results in the periodical change of the transmittance. By the later simulation, it can be shown that the above change will cause the one-way motion of interference fringes.

3.2. Signal detection model

The SNR of the traditional electro-optical detection system [16] can be expressed as:

$$SNR_{trad} = \frac{S_{object}}{\sqrt{S_{object} + N_{sky}}}, \tag{8}$$

In Eq. (8): S_{object} is the photoelectron number generated by the target light and N_{sky} is the photoelectron number generated by the skylight background.

Next, the SNR of the new shearing interference detection system will be analyzed. By the analysis in section 3.1, the intensity distribution of the interference fringes formed by the target light on the detector can be obtained. When grating 2 moves along one direction vertical to the grating lines, the interference fringes will also move in a certain direction. When the width of the interference fringe is similar to the size of the pixel, the detector can convert the fluctuating light intensity of the interference fringes into the periodical electrical signal. The light from the skylight background can't form the interference fringes, which is converted into the random electrical signal by the detector.

According to the above working principle and the assumption of the weak signal detection method given at the beginning of section 3, the output signal after the weak signal detection can be obtained:

$$S_{out-tot} = filter_{f-mod}(F_t(S_{obj-mod} + N_{sky-n})), \tag{9}$$

In Eq. (9): $S_{out-tot}$ is the total output signal which is represented by the amplitude in the temporal-frequency domain corresponding to the modulation frequency; $S_{obj-mod}$ is the periodical electrical signal generated by the target light; N_{sky-n} is the random electrical signal generated by the skylight background; $F_t(\cdot)$ represents the Fourier transform operator in the time domain and $filter_{f-mod}(\cdot)$ represents the narrow-band filtering operation in the frequency domain centered on the modulation frequency.

From the above equations, the output SNR of the new shearing interference detection system [17] can be expressed as:

$$SNR_{shear} = \frac{mean(S_{out-tot})}{std(S_{out-tot})}, \tag{10}$$

In Eq. (10): $mean(\cdot)$ indicates the average of multiple detected values of the total output electrical signal and $std(\cdot)$ indicates the standard deviation of multiple detected values of the total output electrical signal.

Optics EXPRESS

So far, we have shown the mathematical models of two main parts of the new shearing interference detection method. Next, based on the above models, the simulation of the performance of the new detection method will be carried out. By the simulation, we will find that the new detection method has a higher SNR than the traditional detection method, that is, the new detection method has a better performance to suppress the skylight background noise.

4. Simulation and analysis

The purposes of the simulation are to verify the feasibility of the new detection method to suppress the skylight background noise and to achieve a preliminary quantitative comparison of the detection performance between the new detection method and the traditional one. The simulation programming tool is MATLAB software. In order to facilitate the computer simulation, we will show the main parameters used in the simulation, which are shown in Table 1.

Table 1. List of the selected parameters for the simulation.

Main parameter	Value
Wavelength: λ	532nm
Amplitude: A_1	1
Initial phase: φ_0	0
Angle of incidence: θ	0°
Grating period: d	10μm
Distance between gratings 1 and 2	0.38mm
Distance between grating 2 and the detector	0.076mm
Rotation angle of grating 2:ε	3°
Moving step of grating 2	10μm/30
Size of pixels of the detector	Fringe period /2

According to the mathematical model in section 3 and the above main parameters, we have carried out the numerical simulation for the new detection method. The distributions of the interference fringes generated at different moments are shown in Fig. 2. It can be seen that when grating 2 moves in one direction in the grating plane vertical to the grating lines, the Moire fringes on the detector will also move in a certain direction.

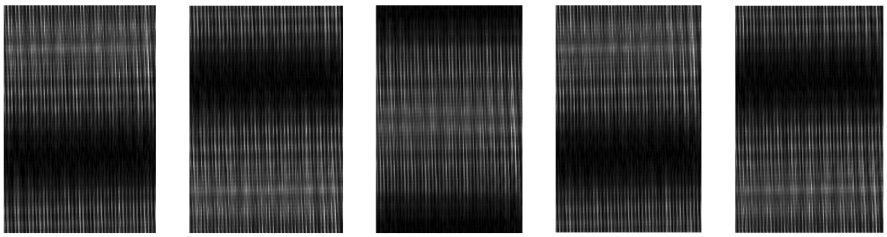

Fig. 2. Distributions of single period interference fringe at different time. (a), (b), (c), (d) and (e) correspond to the distribution of a single period fringe when t = (1/5) period, (2/5) period, (3/5) period, (4/5) period, 1 period, respectively. The above period is the temporal period of the fringe motion.

The output electrical signal (no noise) generated by the Moire fringes scanning across the detector is shown in Fig. 3. In this figure, the ordinate is the normalized signal amplitude and the

Optics EXPRESS

abscissa is the time or the number of motion steps of grating 2. It can be seen that the electrical signal generated by the one-way movement of Moire fringes is approximately sine wave.

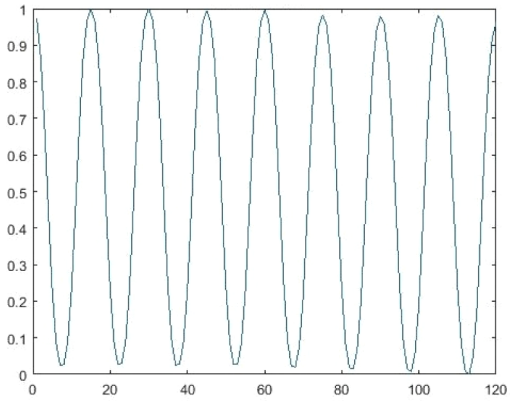

Fig. 3. Output electrical signal (without noises).

The SNR of the traditional electro-optical detection system (its basic structure is shown in Fig. 4) to find the target is generally 3 [18], that is, the mean value (approximately constant value) of the electrical signal generated by the target divided by the standard deviation of the total electrical signal (the sum of the electrical signals generated by the target and the skylight background) is equal to 3. Because the phase modulation is introduced into the target light by the new detection method, the output electrical signal generated by the detector is approximately sine wave. So the mean value of the signal should be replaced with the amplitude of the signal (the amplitude of the sine wave) in the numerator of the above SNR expression, when calculating the SNR of the new detection method. In the simulation, the Gaussian white noise generating function in MATLAB (AWGN) is used to add the noise to the electrical signal generated by the target, which represents the influence of skylight background on the detection performance.

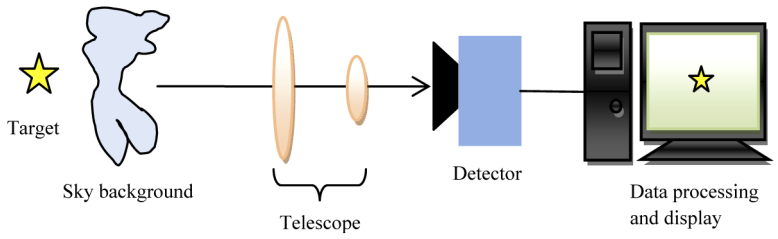

Fig. 4. Basic structure of the traditional detection system.

Comparing Fig. 1 with Fig. 4, we can find that the main structural difference between the new system and the traditional system is that the shearing interferometer composed of two gratings is added to the new system. Assuming that the average transmittance of the shearing interferometer for the target light and the skylight background is the same (about 32%), then according to Eq. (8), the SNR of the new system (marked as $SNR_{shear-in}$, without the phase modulation) is about 57% of that of the traditional system. That is to say, when the SNR of the traditional system (marked as SNR_{trad}) is equal to 1, the input SNR (without the phase modulation) of the new system is about 0.57.

The output electrical signal of the traditional system after adding the Gaussian white noise ($SNR_{trad} = 1$) and its power spectrum are shown in Fig. 5 and Fig. 6, respectively. Figure 5 shows

Optics EXPRESS

that the target signal has been submerged by the noise. Figure 6 shows that since the target light is not modulated, it is difficult to find the difference between the target light and the skylight background in the frequency domain. So it is difficult to extract the target signal by the traditional electro-optical detection system.

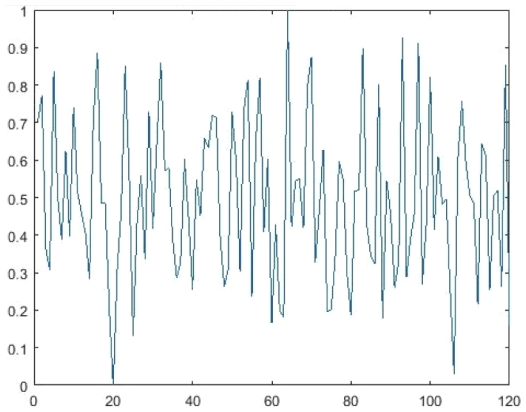

Fig. 5. Output electrical signal of the traditional system.

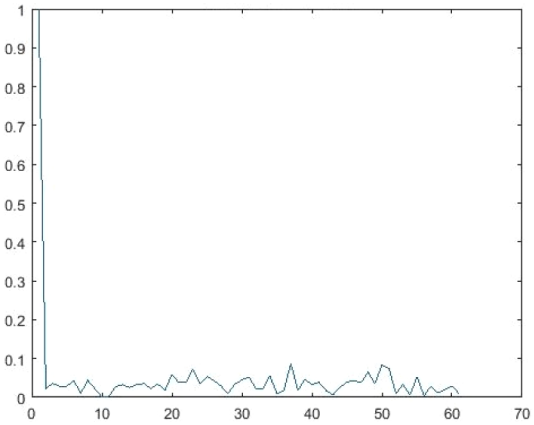

Fig. 6. Power spectrum of the traditional system.

The output electrical signal of the new system (with the phase modulation) after adding the Gaussian white noise ($SNR_{shear-in} = 0.57$) and its power spectrum are shown in Fig. 7 and Fig. 8, respectively. Figure 7 shows that the modulated target signal has been submerged by the noise and that the periodical structure of the signal can't be distinguished. Figure 8 shows that the discrepancy in the frequency domain between the target light and the skylight background can still be distinguished when the input SNR is very low. According to Eq. (12) given above, the output SNR of the new shearing interference detection system can be calculated to be about 2.99. It can be seen that compared with the input SNR, the output SNR is significantly improved (about 5 times of the input SNR).

The results with or without the target obtained by narrow-band filtering in the frequency domain are shown in Fig. 9. According to Fig. 9, it can be seen that the combination of the optical interference and the weak signal detection (narrow-band filtering in the frequency domain) can effectively detect dim targets in the strong noises. In the practical case, the area array detector is

Optics EXPRESS

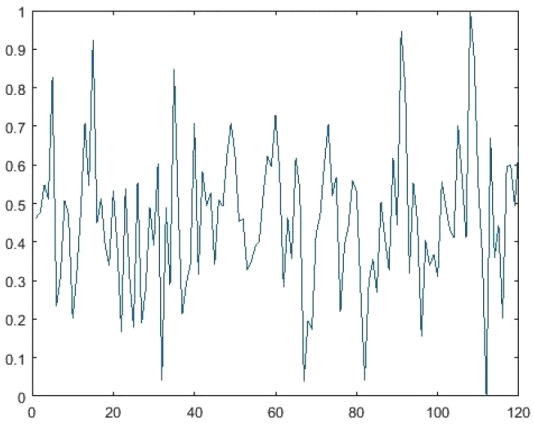

Fig. 7. Output electrical signal of the new system.

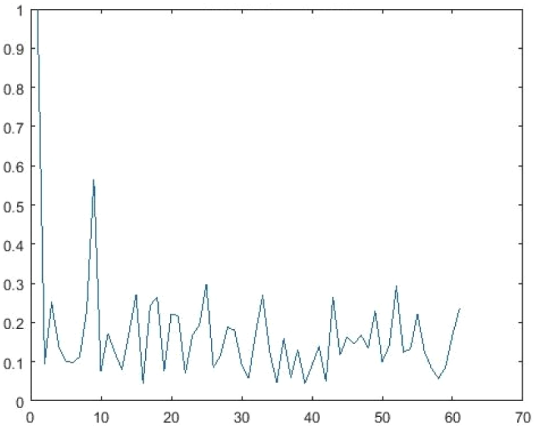

Fig. 8. Power spectrum of the new system.

used. Each pixel of the detector corresponds to a weak signal detection channel and all channels are detected simultaneously. If the target appears in the field of view, the detection value of one pixel of the detector will be far greater than that of other pixels, which indicates that the target does appear in the corresponding position of the field of view.

By the above simulation, we can find that the output SNR of the new shearing interference detection system is obviously better than that of the traditional detection system. When the input SNR of the traditional system equals to 1, it is difficult for the traditional system to find the target, but the new system can still find the target easily (the output SNR is about 3). The weak signal detection method used in the simulation is only the simplest frequency domain filtering method. If we choose a better detection method (such as the correlation detection method based on the lock-in amplifier), the output SNR will be further improved. At this point, we can obtain that the new shearing interference detection system is more suitable for searching and finding the small and dim targets in the strong skylight background in the daytime (the input SNR is no more than 1).

Optics EXPRESS

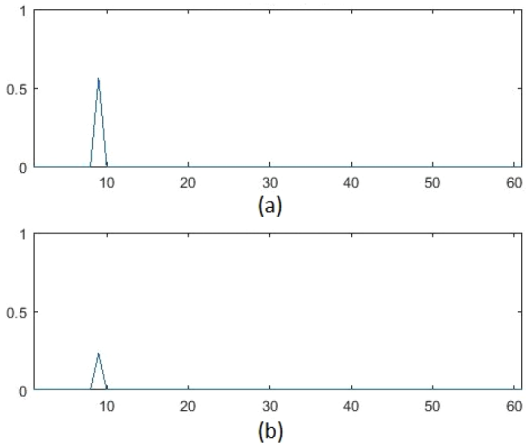

Fig. 9. Results by the narrow-band filtering. (a) and (b) correspond to the results with or without the target, respectively.

5. Conclusion

In this paper, a new detection method based on the shearing interference and the phase modulation has been analyzed and simulated. By analyzing the simulation results and comparing this new detection method with the traditional one, we can obtain the following conclusions.

(I) The new detection method based on the shearing interference and the phase modulation is feasible in principle. Because the shearing amount of the grating shearing interferometer can be continuously adjustable from zero to several centimeters and the spatial coherence length of the skylight background in the far field is about several microns, only a few tens of microns of the shearing amount may be enough to make the skylight background unable to form interference fringes. The contrast of the interference fringes formed with tens of microns of the shearing amount is much greater than that formed with several millimeters of two-aperture separation. Therefore, the new detection method based on the shearing interference and the phase modulation has a better detection performance than the original interference detection method based on two electro-optical modulators. Because the aperture of the beam is at least 1 cm and the two beams produced by the shearing interferometer with only tens of microns of the shearing amount may almost overlap each other, the aperture utilization (the ratio of the overlapping area of the shear beams to the area of the single beam) of the new detection method is close to 100%, far greater than the original interference detection method.

(II) Compared with the input SNR, the output SNR of the new detection method is significantly improved (about 5 times of the input SNR). If a better the weak signal detection method (such as the correlation detection method based on the lock-in amplifier) can be used, the output SNR can be further improved. At this time, the new detection method may still be able to detect the target which can't be detected by the traditional method (the input SNR is no more than 1).

It can be seen that the new detection method has a better performance on suppressing the skylight background and improving the detection probability of the dim target and also has space for further performance improvement. Therefore, this new detection method will provide a powerful technique for the detection of dim targets in the strong skylight background.

Optics EXPRESS

Funding

National Natural Science Foundation of China (11703024).

Acknowledgments

Thank my colleague Shan Jiang for giving some useful advices and help in the computer simulation.

Disclosures

The authors declare no conflicts of interest.

References

1. R. Eixmann, M. Gerding, J. Hoeffner, and M. Kopp, "Lidars with narrow FOV for daylight measurements," IEEE Trans. Geosci. Electron. **53**(8), 4548–4553 (2015).
2. C. C. Evans, D. N. Woolf, J. M. Brown, and J. M. Hensley, "A daytime free-space quantum-optical link using atomic-vapor spectrum filters," *Conference on lasers and electro-optics (CLEO)*, (San Jose, CA, 2019).
3. R. Dungee, M. Chun, and Y. Hayano, "On the feasibility of using a laser guide star adaptive optics system in the daytime," J. Astron. Telesc. Instrum. Syst. **5**(01), 1 (2019).
4. R. Menchon-Enrich, A. Llobera, J. Vila-Planas, V. J. Cadarso, J. Mompart, and V. Ahufinger, "Light spectral filtering based on spatial adiabatic passage," Light: Sci. Appl. **2**(8), e90 (2013).
5. R. Zhang, H. Xian, K. Wei, and C. Rao, "Study on effect of polarization for improving signal noise ratio of stellar objects in daytime," *Proceedings of SPIE, 4th International Symposium on Photoelectronic Detection and Imaging (ISPDI) - Sensor and Micromachined Optical Device Technologies*, (Beijing, Peoples R. China, 2011), 8191, 81911M.
6. A. Basiri, X. Chen, J. Bai, P. Amrollahi, J. Carpenter, Z. Holman, C. Wang, and Y. Yao, "Nature-inspired chiral metasurfaces for circular polarization detection and full-Stokes polarimetric measurements," Light: Sci. Appl. **8**(1), 78 (2019).
7. D. N. Held, "Interferometric daylight star tracker," US3626192[P], 1971-12-07.
8. M. Born and E. Wolf, *Principles of Optics: Electromagnetic Theory of Propagation, Interference and Diffraction of Light* (Cambridge Univ. Press, 1999).
9. J. I. Jimenez-Aquino, N. Sanchez-Salas, L. Ramirez-Piscina, and M. Romero-Bastida, "Unstable state decay in non-Markovian heat baths and weak signals detection," Phys. A (Amsterdam, Neth.) **529**, 121493 (2019).
10. Y. Ling, C. Chen, D. Niu, and T. Chen, "Weak signal detection using double-well Duffing-van der Pol oscillator and formulation of detection statistics," J. Phys. Soc. Jpn. **88**(4), 044001 (2019).
11. J. W. Hardy and A. J. MacGovern, "Shearing interferometry: a flexible technique for wavefront measurement," Proc. SPIE **0816**, 180–195 (1987).
12. L. Zhang, K. Qi, and Y. Xiang, "Two-step algorithm for removing the rotationally asymmetric systemic errors on grating lateral shearing interferometer," Opt. Express **26**(11), 14267–14277 (2018).
13. T. Ling, D. Liu, X. Yue, Y. Yang, Y. Shen, and J. Bai, "Quadriwave lateral shearing interferometer based on a randomly encoded hybrid grating," Opt. Lett. **40**(10), 2245–2248 (2015).
14. B. Lam and C. Guo, "Complete characterization of ultrashort optical pulses with a phase-shifting wedged reversal shearing interferometer," Light: Sci. Appl. **7**(1), 30 (2018).
15. H. Schreiber, P. Dewa, M. Dunn, R. Hordin, S. Mack, B. Statt, and P. Tompkins, "Applications of a Grating Shearing Interferometer at 157 nm," Proc. SPIE **4346**, 1095–1106 (2001).
16. S. R. Restaino and J. R. Andrews, "Comparison of Michelson interferometer, intensity interferometer and filled aperture telescope SNR for GEO satellites detection," Proc. SPIE **8165**, 81650R (2011).
17. F. Roddier, "Interferometric imaging in optical astronomy," Phys. Rep. **170**(2), 97–166 (1988).
18. I. Tcherniavski, "Possibility of detection of Earth-like exo-planets and recognition of their surface areas with a hypertelescope," Opt. Eng. **53**(2), 023106 (2014).